ORIGINAL RESEARCH

Isomeric structures of benzimidazole, benzoxazole, and benzothiazole derivatives, their electronic properties and transformations

Akapong Suwattanamala · Vithaya Ruangpornvisuti

Abstract The optimized structures of all isomers of HBI, HBO, HBT, HPyBI, HPyBO, and HPyBT compounds were obtained using the potential energy surface method at the B3LYP/6-311++G(d,p) level of theory. Four isomers and three transition states of their transformations for each compound of HBO, HBT, HPyBO, and HPyBT and two isomers and one transition state for each HBI and HPyBI compounds were found. Energetics, thermodynamic properties, rate constants, and equilibrium constants of their transformations were determined.

Introduction

Intramolecular proton transfer has played an important role in a large variety of chemical and biological processes. Some types of organic materials undergoing excited state intramolecular proton transfer (ESIPT) have been applied as molecular photoswitches [1], laser dyes and light

A. Suwattanamala
Department of Chemistry and Center of Excellence
for Innovation in Chemistry, Faculty of Science, Burapha
University, Chonburi 20131, Thailand

V. Ruangpornvisuti (✉)
Department of Chemistry, Faculty of Science and Center
for Petroleum, Petrochemicals and Advanced Materials,
Chulalongkorn University, Bangkok 10330, Thailand
e-mail: vithaya.r@chula.ac.th

emitting device [2], UV photostabilizers [3], fluorescent probes [4], or probes for structural variations in micelles [5, 6]. The chemical structure of ESIPT molecules usually contains a phenolic group which is able to form intramolecular hydrogen bond with a heteroatom, such as oxygen or nitrogen in the same molecule. The ESIPT compounds such as 2-(2′-hydroxyphenyl)benzimidazole (HBI) [7–10], 2-(2′-hydroxyphenyl)benzoxazole (HBO) [7, 8, 10–17], and 2-(2′-hydroxyphenyl)benzothiazole (HBT) [10, 14, 18–21] denoted as HBX compound series, where –X– in the benzazole ring standing for –NH–, –O– and –S– were widely studied. Especially, HBO has been explored as a phototautomerizable model DNA base pair [15–17]. The analogs of HBX denoted as HPyBX series are composed of 2-(3′-hydroxy-2′-pyridyl)benzimidazole (HPyBI) [22], 2-(3′-hydroxy-2′-pyridyl)benzoxazole (HPyBO) [23], and a novo 2-(3′-hydroxy-2′-pyridyl)benzothiazole (HPyBT), see Fig. 1. It shows that the ESIPT molecules in the ground state can occur in enol form, called a syn normal form (N_{syn}) possessing the hydroxyl group which is hydrogen-bonded to its N_1 atom via N···H interaction as demonstrated in Fig. 1. The hydroxyl proton of the syn normal form can be transferred to afford its keto tautomer called a syn tautomer (T_{syn}) possessing the intramolecular hydrogen bond, N_1–H···O. The ground state rotamerism yields an anti rotamer form (N_{anti}) and it might reveal a conformational equilibrium between an intramoleculary hydrogen bonded conformer and the OH-rotated conformer (N'_{anti}) (Fig. 1). Ab initio calculations on the N_{syn} and T_{syn} forms of the HBX series and their corresponding transition states (**TS**) were carried out by previous theoretical studies [10, 13] but unfortunately, no physical insights on thermodynamic and kinetic parameters were obtained.

In this work, the structural details of each form of HBX and HPyBX series of benzimidazole, benzoxazole, and

Fig. 1 Structural representatives for six compounds of ESIPT as (four forms N_{syn}, T_{syn}, N_{anti}, and N'_{anti}) the X, Y-substituted molecular series

benzothiazole derivatives and their corresponding transition states in tautomeric and rotameric transformations using DFT/B3LYP calculations have been investigated. In the gas phase, thermodynamic and kinetic parameters of each process have been determined.

Computational details

The structures of HBX and HPyBX compounds, X = –NH–, –O– and –S– and their related transition states in tautomerism and rotamerism were obtained by complete optimization using density functional theory (DFT). DFT calculations were performed by the Becke's three-parameter exchange functional [24] combined the Lee–Yang–Parr correlation functional [25] (B3LYP). All geometry optimizations were carried out using the computation at the B3LYP/6-311++G(d,p) level of theory. All minima and transition states were confirmed by real and single imaginary vibrational frequencies, respectively. All calculations were performed with the GAUSSIAN 03 program [26].

The Mulliken electronegativity (χ), chemical hardness (η), and electronic chemical potential (μ) for all isomers of the HBX and HPyBX compounds were computed using orbital energies of the highest occupied molecular orbital (HOMO) and the lowest unoccupied molecular orbital (LUMO) at the B3LYP/6-311++G(d,p) level. The chemical hardness, electronic chemical potential, and Mulliken electronegativity were derived from the first ionization potential (I) and electron affinity (A) of the N-electron molecular system with a total energy (E) and external potential ($v(\vec{r})$) using the relations: $\chi = -\left(\frac{\partial E}{\partial N}\right)_{v(\vec{r})} = -\mu \cong \frac{1}{2}(I+A)$ and $\eta = \left(\frac{\partial^2 E}{\partial N^2}\right)_{v(\vec{r})} \cong \frac{1}{2}(I-A)$, and the

first ionization potential and electron affinity are $I = E(N-1) - E(N)$ and $A = E(N) - E(N+1)$, respectively [27]. According to the Koopmans theorem [28], I and A were computed from the HOMO and LUMO energies using the relations: $I = -E_{HOMO}$ and $A = -E_{LUMO}$, as employed in the previous works [29–37].

The standard enthalpy ΔH^o_{298} and Gibbs free energy changes ΔG^o_{298} of tautomeric and rotameric reactions of this system have been derived from the frequency calculations at the B3LYP/6-311++G(d,p) level of theory; no scaled frequency is used. The rate constant $k(T)$, based on transition state theory, was computed from the activation energy, $\Delta^{\ddagger}E$ using Eq. 1.

$$k(T) = \kappa \frac{k_B T}{h} \frac{Q_{TS}}{Q_{REA}} \exp\left(-\Delta^{\ddagger}E/RT\right)$$
$$= \kappa A \exp\left(-\Delta^{\ddagger}E/RT\right) \tag{1}$$

where k_B is the Boltzmann's constant, h is Planck's constant, T is the absolute temperature, R is the gas constant, and Q_{TS} and Q_{REA} are the partition functions of the transition state and the isomeric reactant of HBX and HPyBX molecules whose values are composed of translational, rotational, and vibrational partition functions. The tunneling coefficient (κ) can be computed with the Wigner method [38–40] as $\kappa = 1 + \frac{1}{24}\left(\frac{h v_i}{k_B T}\right)^2$ where v_i is the imaginary frequency that accounts for the vibration motion along the reaction path. The pre-exponential factor (A) is defined as $A = \frac{k_B T}{h} \frac{Q_{TS}}{Q_{REA}}$. The equilibrium constant K at 298.15 K and 1 atm is computed using a thermodynamic equation $\Delta G^o = -RT \ln K$.

Results and discussion

Structure and energetics of each isomer of HBX and HPyBX series

The B3LYP/6-311++G(d,p) optimized structures of ground state isomers N_{syn}, T_{syn}, N_{anti} and N'_{anti} of HBx and HPyBx series and their corresponding transition states of their tautomerization and rotamerization are shown in Figs. 2, 3, 4, 5, 6, and 7. The optimized structures of isomer N_{syn} of HBx and HPyBx series were found to be planar which corresponds to previous study on HBX group [10]. By the way, the proton can be transferred from the hydroxyl group to the benzazole N_1 and yield the T_{syn} with strong O···H interaction. Rotameric equilibria in the ground state between N_{syn} and its anti rotamer N_{anti} and between N_{anti} and N'_{anti} rotamer were found for all systems except for HBI and HPyBI compounds.

Only two isomers of HBI, NC, and NC′ were found and they transform each other via transition state TS_NC′_NC′

Fig. 2 The structures of isomers of HBI compound, their transformations via transition states as **a** without and **b** with water-assisted proton-transfer process. Hydrogen bond distances are in angstrom. Imaginary frequency for their transition states are shown in parentheses
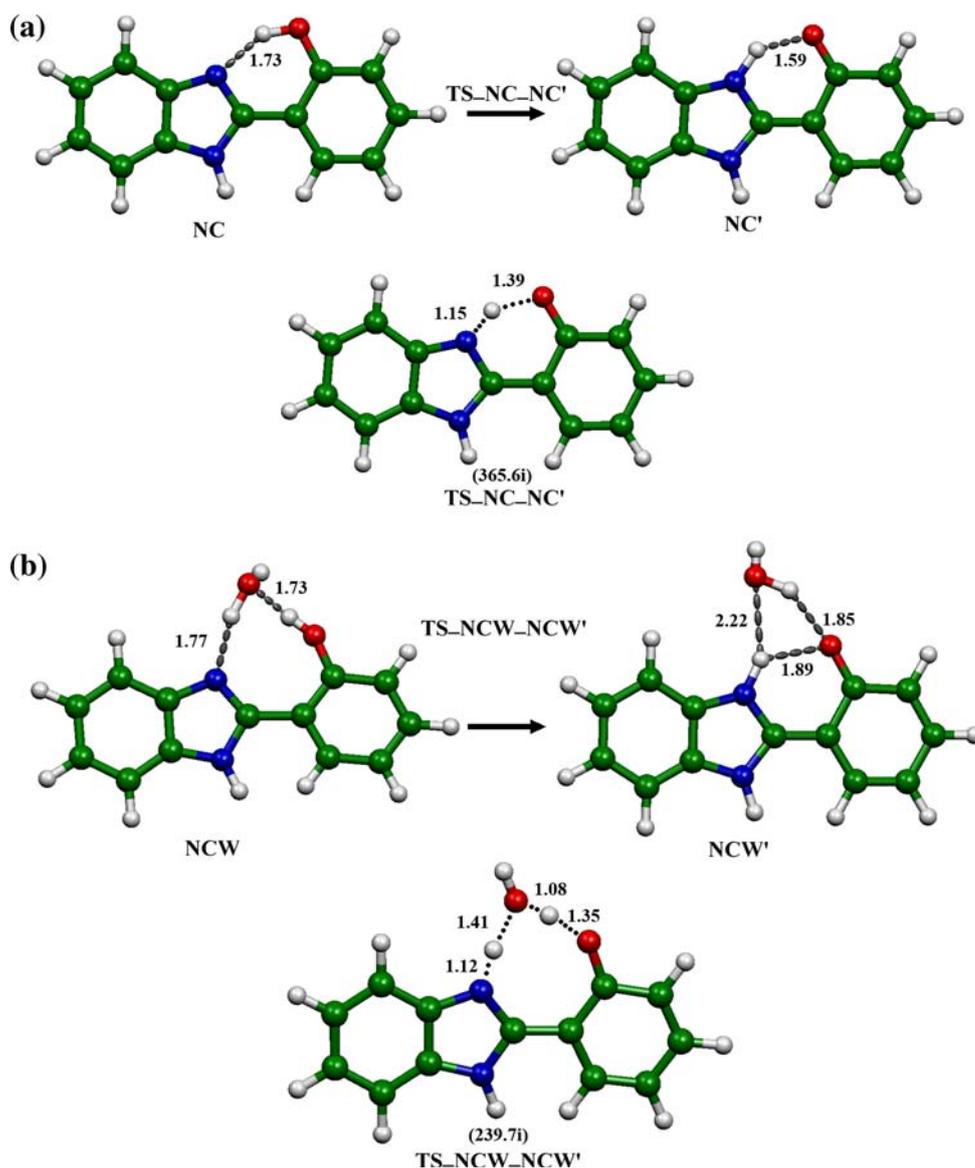
as shown in Fig. 2; their transformation as proton transfer via a water molecule is shown in Fig. 2b. Four conformers N_{syn}, T_{syn}, N_{anti}, and N'_{anti} denoted as OC, OC′, OC″, and OC‴ for HBO compound and as SC, SC′, SC″, and SC‴ for HBT compound including their transformations are shown in Figs. 3 and 4, respectively. Two isomers of the HPyBI compound can be transformed into each other via transition state TS_NN_NN′ as shown in Fig. 5. As the C atom in phenolic ring is substituted with N atom, the N-substituted phenolic ring affect the C2–Y bond length and therefore the C2–N is shorter than C2–C by 0.80 Å. The four isomers of the HPyBO and HPyBT compounds can be transformed into each other as the same of the HBO compound as shown in Figs. 6 and 7, respectively.

Selected geometrical parameters of all isomers of the HBX and HPyBX series obtained at the B3LYP/6-311++G(d,p) level of theory are given in Tables S1, S2,

S3, S4, S5, and S6. They show that the C1–X bond distances in HBT are hardly different compared with the isomers of HBI compound but are longer than of HBO by approximately 0.40 Å. The N1–C1–C2–C3 dihedral angles in Tables S3 and S6 show that SC″ and ON″ isomers are a distorted planar structure. Relative energies of isomers of the HBX and HPyBX series and their corresponding transition states of their transformations computed at the B3LYP/6-311++G(d,p) level in gas phase are shown in Table 1. The relative stabilities of isomers of the HBO compound are in order: OC > OC″ > OC‴ > OC′, whereas of the HBT compound are in order: SC > SC‴ > SC″ > SC′. By contrast, the relative stabilities of isomers of the HPyBO compound were found to be in order: ON > ON″ > ON′ > ON‴, whereas of HPyBT compound are in order: SN > SN′ > SN″ > SN‴. The results indicate that the substitution on one C atom by N

Fig. 3 The structures of isomers of HBO compound, their transformations via transition states as **a** without and **b** with water-assisted proton-transfer process. Hydrogen bond distances are in angstrom. Imaginary frequency for their transition states are shown in parentheses
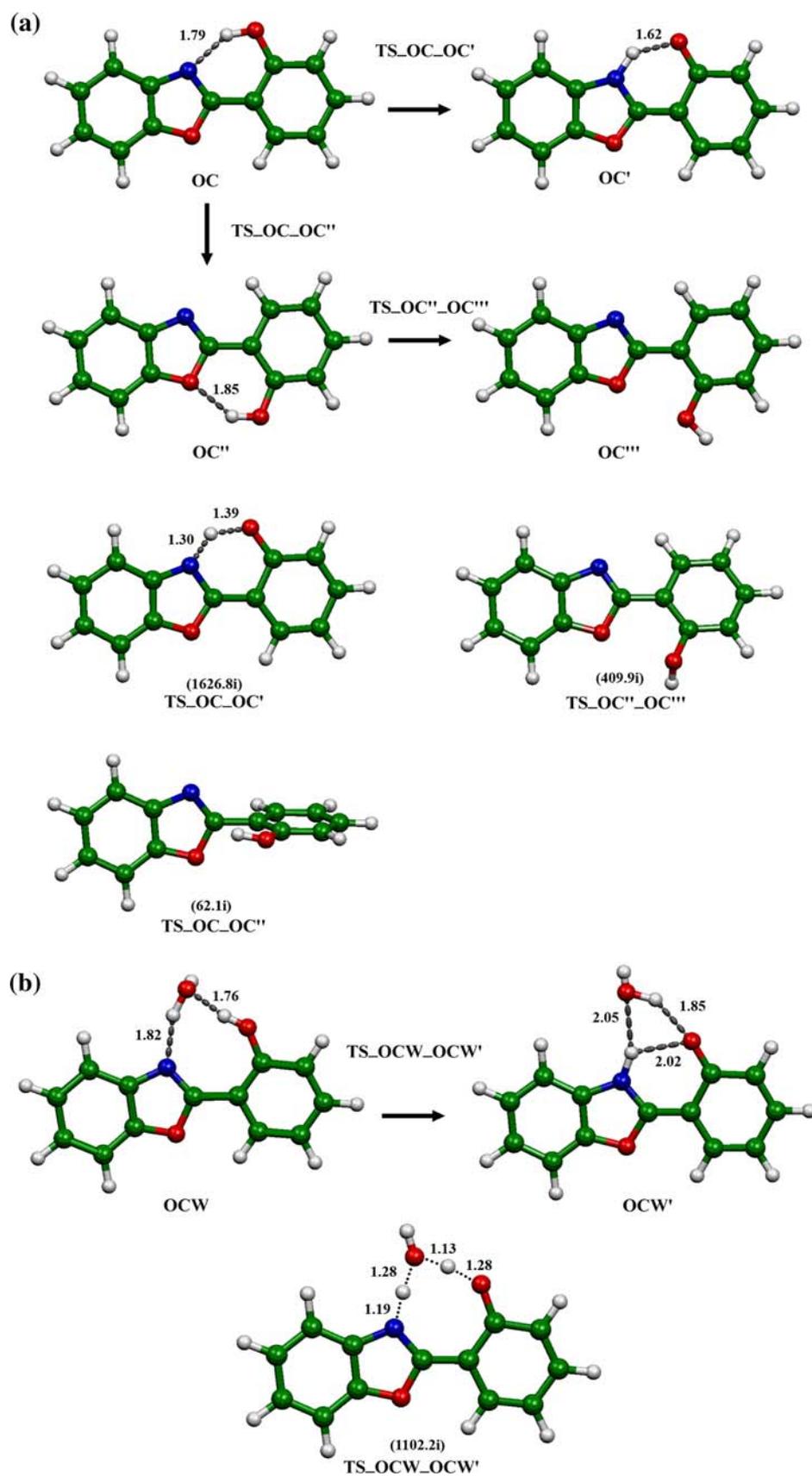
Fig. 4 The structures of isomers of HBT compound, their transformations via transition states as **a** without and **b** with water-assisted proton-transfer process. Hydrogen bond distances are in angstrom. Imaginary frequency for their transition states are shown in parentheses
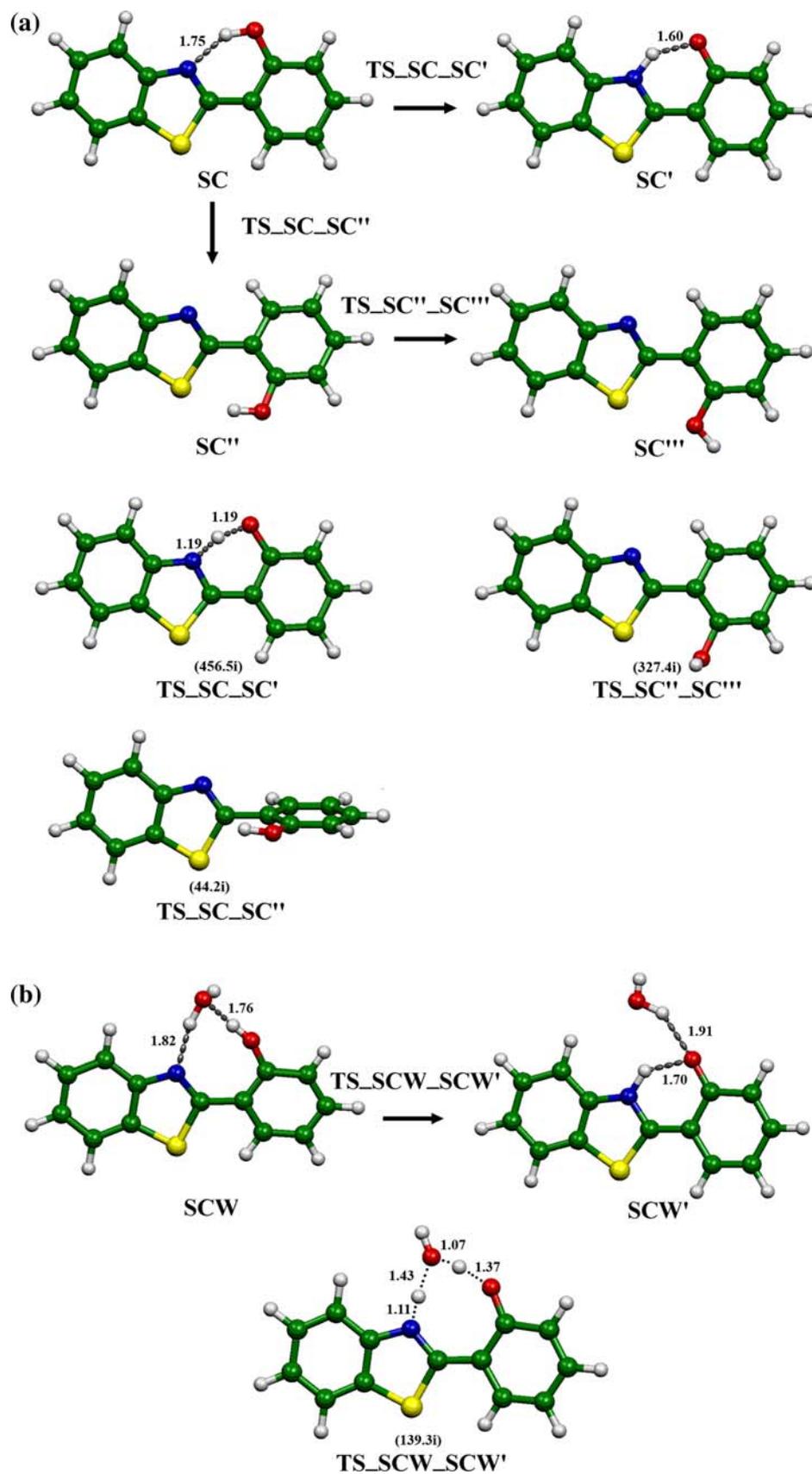
Fig. 5 The structures of isomers of HPyBI compound, their transformations via transition states as **a** without and **b** with water-assisted proton-transfer process. Hydrogen bond distances are in angstrom. Imaginary frequency for their transition states are shown in parentheses
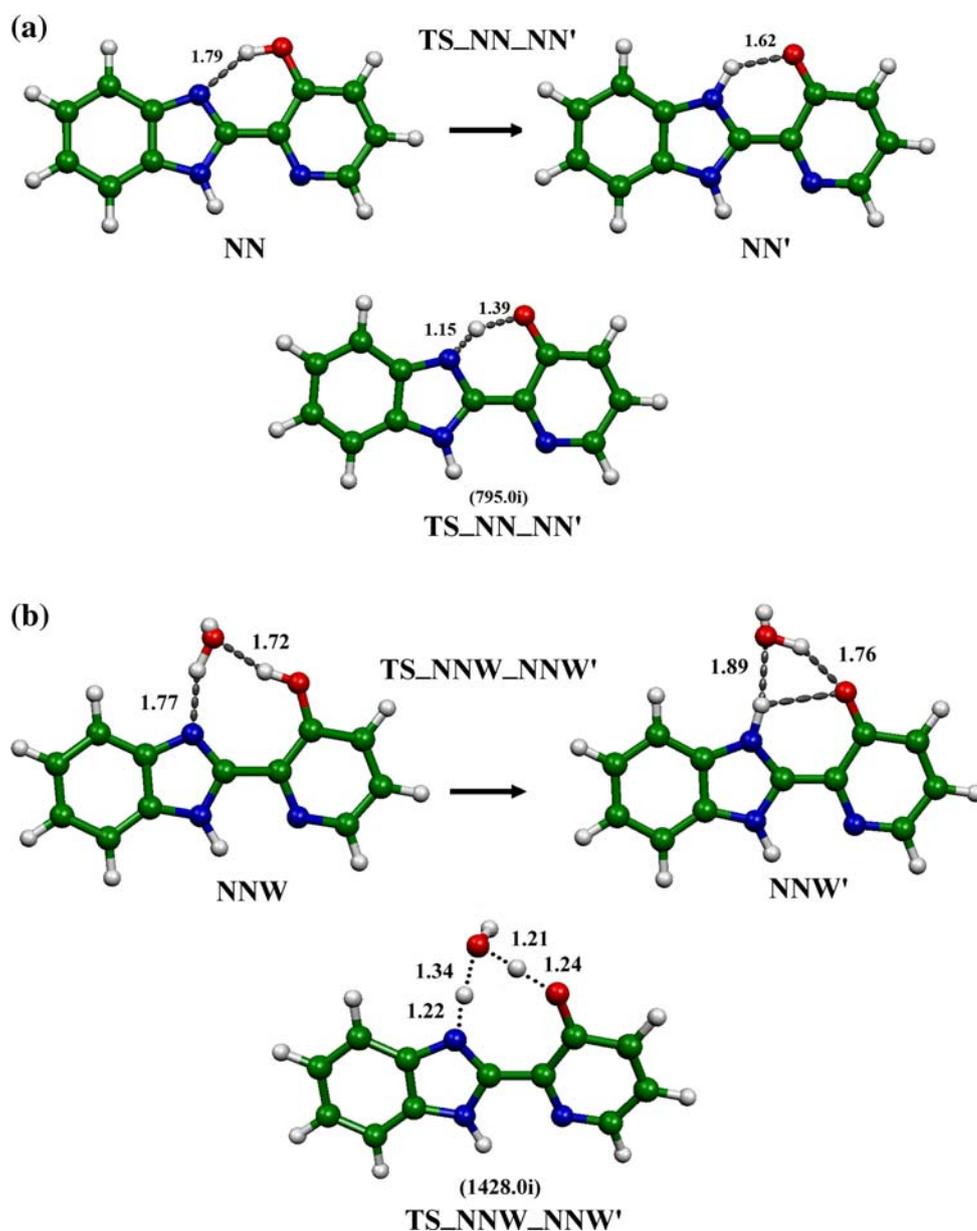
atom in phenolic ring affects the stability ordering of ESIPT compounds. The relative stabilities of HPyBI are predicted as in order: NN > NN′, which corresponds to a previous stability ordering of HBI, NC > NC′. It was found that the N···HO intramolecular hydrogen bond of N_{syn} isomers play an important role in the stabilization of their structures.

Thermodynamic and kinetic properties
of tautomerization and rotamerization

The activation energies, free energies of activation, reaction enthalpies, free energies of reactions, rate constants,

and equilibrium constants of all the tautomerizations and rotamerizations of HBX and HPyBX series obtained at the B3LYP/6-311++G(d,p) level are listed in Table 2. The rate constants of all related reactions computed using Eq. 1 of which rate constant depends on the tunneling coefficient as a part of pre-exponential factor and the activation energy as the exponential part can be considered in terms of imaginary frequencies of their transition state and their corresponding activation energy.

The imaginary frequencies of transition states due to their proton-transfer process such as TS_OC_OC′, 1262.8i cm^{-1} (TS_OCW_OCW′, 1102.2i cm^{-1}, as a system for water-assisted proton transfer, see Fig. 3) and TS_NN_NN′,
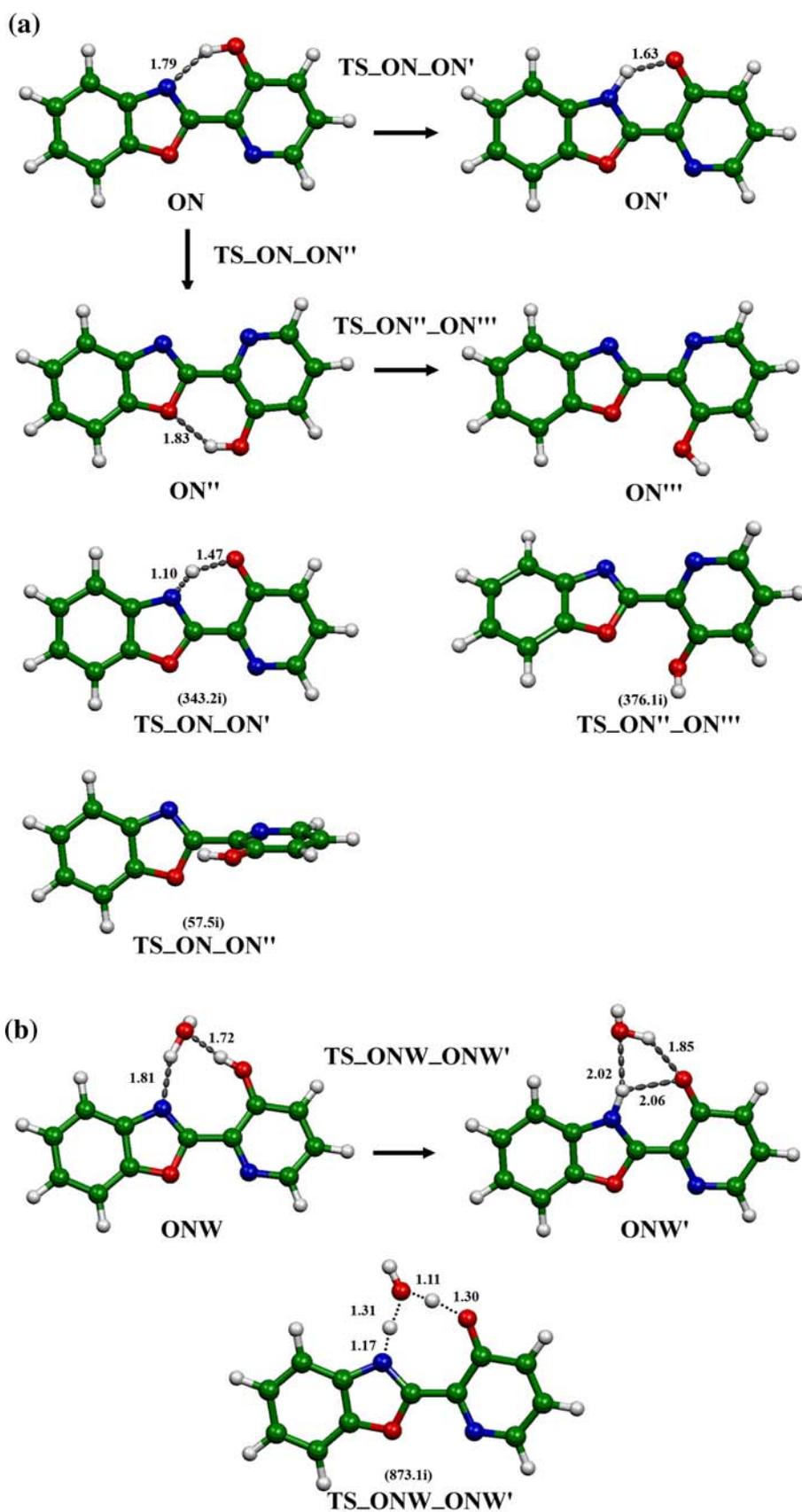
Fig. 7 The structures of isomers of HPyBT compound, their transformations via transition states as **a** without and **b** with water-assisted proton-transfer process. Hydrogen bond distances are in angstrom. Imaginary frequency for their transition states are shown in parentheses
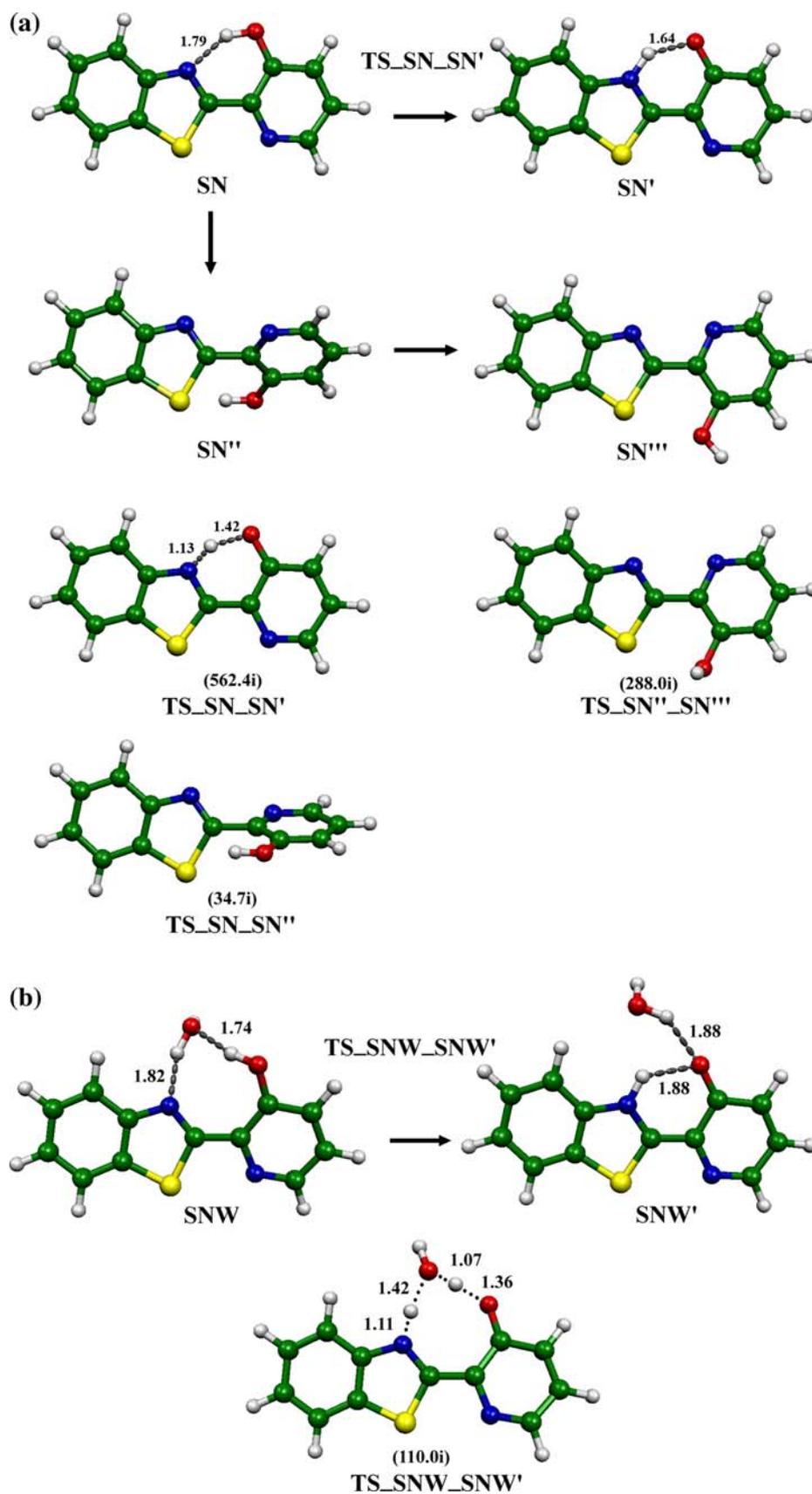
Table 1 Relative energy (ΔE^a) of conformer of the HBX and HPyBX series and transition states of their transformations and relative energy with zero-point energy correction (ΔE^a_{ZPE} in parenthesis) computed at B3LYP/6-311++G(d,p) level in gas phase

Compounds/Isomers	ΔE (kcal/mol)	
	Bare structure	Monohydrated structure
HBI		
NC	0.00 (0.00)	0.00 (0.00)
NC'	9.47 (8.32)	3.00 (2.32)
TS_NC_NC'	9.53 (7.22)	9.64 (7.14)
HBO		
OC	0.00 (0.00)	0.00 (0.00)
OC'	12.68 (11.44)	5.04 (4.67)
OC''	5.64 (5.42)	
OC'''	10.94 (10.32)	
TS_OC_OC'	25.69 (21.51)	13.37 (9.83)
TS_OC_OC''	13.31 (12.64)	
TS_OC''_OC'''	14.06 (12.95)	
HBT		
SC	0.00 (0.00)	0.00 (0.00)
SC'	10.73 (9.70)	2.92 (2.03)
SC''	9.27 (9.02)	
SC'''	8.53 (8.03)	
TS_SC_SC'	10.53 (7.67)	11.52 (9.45)
TS_SC_SC''	11.11 (10.63)	
TS_SC''_SC'''	11.76 (10.77)	
HPyBI		
NN	0.00 (0.00)	0.00 (0.00)
NN'	8.51 (8.02)	0.84 (0.97)
TS_NN_NN'	9.34 (6.76)	11.11 (6.99)
HPyBO		
ON	0.00 (0.00)	0.00 (0.00)
ON'	11.34 (10.19)	4.13 (3.85)
ON''	7.85 (7.50)	
ON'''	14.13 (13.28)	
TS_ON_ON'	11.40 (9.11)	12.13 (8.77)
TS_ON_ON''	13.33 (12.61)	
TS_ON''_ON'''	16.28 (15.03)	
HPyBT		
SN	0.00 (0.00)	0.00 (0.00)
SN'	9.81 (8.95)	1.90 (1.67)
SN''	14.93 (14.46)	
SN'''	16.14 (15.28)	
TS_SN_SN'	10.04 (7.56)	10.50 (8.74)
TS_SN_SN''	15.20 (14.61)	
TS_SN''_SN'''	18.80 (17.59)	

[a] Relative energy to the most stable form (N_{syn}). The most stable form, its total energy is -686.346174, -706.207810, -1029.184884, -702.394815, -722.245682 au. for NC, OC, SC, NN, ON, SN, respectively, calculated at the B3LYP/6-311++G(d,p) whereas the most stable species of monohydrated form, its total energy is -762.807729, -782.667693, -1105.644097, -778.856481, -798.706181, -798.706181 au. for NC, OC, SC, NN, ON, SN, respectively, calculated at the B3LYP/6-311++G(d,p)

795.0i cm^{-1} (TS_NNW_NNW', 1428.0i cm^{-1}, see Fig. 5) highly affect their tunneling coefficients of which are 3.57 (2.18, for water-assisted proton transfer) and 1.61 (2.98, for water-assisted proton transfer), respectively. In general, vibration of transition state is found that its single imaginary frequency for proton-transfer process is usually much higher than that for rotational process. In this work, the imaginary frequency for proton-transfer of the transition state of all studied compounds are lower than 500i cm^{-1} except the reaction for HBO compound (OC $\rightarrow$ TS_OC_OC' $\rightarrow$ OC', 1626.8i cm^{-1}) and for HPyBI (NN $\rightarrow$ TS_NN_NN' $\rightarrow$ NN', 795.0i cm^{-1}). Reasons of the low vibration frequencies for these proton-transfer transition states are that they possess high intramolecular repulsive site as described below:

- HBI system, the transition state TS_NC_NC' (Fig. 2) is caused by the interaction [ring–NH↔HC–ring].
- HBT system, the transition state TS_SC_SC' (Fig. 4) is caused by the ring strain due to the sulfur atom.
- HPyBO system, the transition state TS_NC_NC' (Fig. 6) is caused by the interaction [ring–O↔N–ring].
- HPyBT system, the transition state TS_NC_NC' (Fig. 7) is caused by the interaction [ring–S↔N–ring].

Intramolecular proton transfer reactions of all members in the HBX and HPyBX series are the non-spontaneous and endothermic processes, which is supported by positive values of both free energy change, ΔG^o_{298}, and enthalpy change, ΔH^o_{298}, of the reaction. The reaction enthalpies for HBX series are predicted to be in order: HBI < HBT < HBO, which is in good agreement with the previous theoretical study [10]. It was found that these results follow the Leffer–Hammond postulate [41, 42]. In the same manner, reaction enthalpies for HPyBX series are found to be in order: HPyBI < HPyBT < HPyBO. It seems that the substitution on C atom in phenolic ring for HBX series by N atom (HPyBX series) does not break the Leffer–Hammond postulate because this substitution does not affect to the proton transfer process.

Activation energies for tautomerization of the HBX and HPyBX series are in increasing order: NN $\rightarrow$ TS_NN_NN' < NC $\rightarrow$ TS_NC_NC' < SN $\rightarrow$ TS_SN_SN' < SC $\rightarrow$ TS_SC_SC' < ON $\rightarrow$ TS_ON_ON' < OC $\rightarrow$ TS_OC_OC'. It might suggest that reaction enthalpies and activation energies for the tautomerization of compounds in HPyBX series are lower than their corresponding compounds in HBX series. It suggests that the activation energy for the tautomerization increases with decreasing hydrogen bond strength. This suggestion is supported by hydrogen bond distance H···N in N_{syn} and transition-state structures. On the other hand, the activation energy seems to increase with the increasing electronegativity of X substituted compounds. The rate constants and equilibrium constants at

Table 2 Energies, thermodynamic properties, rate constants and equilibrium constants of transformations of all isomers of the HBX and HPyBX series computed at the B3LYP/6-311++G(d,p) level of theory

Reactions /systems	$\Delta^{\ddagger}E$ [a, b]	$\Delta^{\ddagger}G$ [a]	ΔE [a, b]	ΔH [a]	ΔG [a]	κ [c]	A [d]	k_{298} [e]	K_{298}
HBI									
NC → TS_NC_NC' → NC'	7.22	7.75	8.32	8.37	8.48	1.13	2.49×10^{12}	1.43×10^{7}	6.08×10^{-7}
NCW → TS_NCW_NCW' → NCW'	7.14	7.81	2.32	2.80	1.43	1.06	2.00×10^{12}	1.22×10^{7}	8.89×10^{-2}
HBO									
OC → TS_OC_ OC' → OC'	21.51	22.13	11.44	11.51	11.46	3.57	2.19×10^{12}	1.33×10^{-3}	3.95×10^{-9}
OCW → TS_OCW_ OCW' → OCW'	9.83	10.79	4.67	4.93	4.40	2.18	1.17×10^{12}	1.60×10^{5}	5.92×10^{-4}
OC → TS_OC_ OC'' → OC''	12.64	12.97	5.42	5.57	5.10	1.00	3.55×10^{12}	1.93×10^{3}	1.83×10^{-4}
OC'' → TS_OC''_ OC''' → OC'''	7.53	7.43	4.90	5.10	4.02	1.16	7.46×10^{12}	2.61×10^{7}	1.13×10^{-3}
HBT									
SC → TS_SC_ SC' → SC'	7.67	7.70	9.70	9.79	9.77	1.20	5.81×10^{12}	1.67×10^{7}	6.92×10^{-8}
SCW → TS_SCW_ SCW' → SCW'	9.45	9.43	2.03	2.44	1.29	1.02	6.31×10^{12}	7.54×10^{5}	1.13×10^{-1}
SC → TS_SC_ SC'' → SC''	10.63	11.15	9.02	9.20	8.78	1.00	2.58×10^{12}	4.17×10^{4}	3.64×10^{-7}
SC'' → TS_SC''_ SC''' → SC'''	1.75	1.87	−0.99	−0.87	−1.19	1.10	5.09×10^{12}	2.93×10^{11}	7.41×10^{0}
HPyBI									
NN→ TS_NN_NN' → NN'	6.76	7.08	8.02	8.07	8.01	1.61	3.54×10^{12}	6.29×10^{7}	1.34×10^{-6}
NNW→ TS_NNW_NNW' → NNW'	6.99	8.75	0.97	1.12	1.26	2.98	3.07×10^{11}	6.85×10^{6}	1.20×10^{-1}
HPyBO									
ON→ TS_ON_ON' → ON'	9.11	9.53	10.19	10.25	10.21	1.11	3.02×10^{12}	7.06×10^{5}	3.29×10^{-8}
ONW→ TS_ONW_ONW' → ONW'	8.77	9.51	3.85	4.13	3.59	1.74	1.71×10^{12}	1.11×10^{6}	2.34×10^{-3}
ON→ TS_ON_ON'' → ON''	12.61	12.91	7.50	7.66	7.04	1.00	3.79×10^{12}	2.15×10^{3}	6.91×10^{-6}
ON''→ TS_ON''_ON''' → ON'''	7.53	7.48	5.79	5.43	6.75	1.14	6.82×10^{12}	2.33×10^{7}	1.13×10^{-5}
HPyBT									
SN→ TS_SN_SN' → SN'	7.56	7.91	8.95	8.99	8.98	1.31	3.37×10^{12}	1.27×10^{7}	2.62×10^{-7}
SNW→ TS_SNW_SNW' → SNW'	8.74	9.16	1.67	1.96	1.33	1.01	2.92×10^{12}	1.16×10^{6}	1.06×10^{-1}
SN→ TS_SN_SN'' → SN''	14.61	14.97	14.46	14.71	13.84	1.00	3.42×10^{12}	6.65×10^{1}	7.16×10^{-11}
SN''→ TS_SN''_SN''' → SN'''	3.13	3.37	0.82	0.97	0.04	1.08	4.17×10^{12}	2.28×10^{10}	9.31×10^{-1}

[a] In kcal/mol

[b] Energy with zero-point vibration energy (ZPVE) corrections

[c] $\kappa = 1 + \frac{1}{24}\left(\frac{h\nu_i}{k_B T}\right)^2$

[d] $A = \frac{k_B T}{h}\frac{Q_{TS}}{Q_{REA}}$ in s^{-1}

[e] In s^{-1}

298.15 K of tautomerization processes are in orders: NN → NN' > SC → SC' > NC → NC' > SN → SN' > ON → ON' > OC → OC' and NN → NN' > NC → NC' > SN → SN' > SC → SC' > ON → ON' > OC → OC', respectively. All the equilibrium constants at 298.15 K of tautomerization processes via transition-state geometry corresponding to water-assisted proton transfer are higher than their corresponding equilibrium constants obtained via direct proton-transfer process by 10^4 times.

All the first rotameric transformation ($N_{syn} \rightarrow N_{anti}$) and second rotameric transformation ($N_{anti} \rightarrow N'_{anti}$) are endothermic and non-spontaneous reactions except the second rotameric transformation SC'' → SC''' which prefers undergo the exothermic and spontaneous process; its enthalpy and free energy are small magnitude, $\Delta H = -0.87$ kcal/mol and $\Delta G = -1.19$ kcal/mol. As all these

forward rate constants are very small as compared with their corresponding backward rate constants, their reaction equilibrium constants are therefore small; although the equilibrium constant of the transformation SC'' → SC''' is also small ($K = 7.41 \times 10^0$) as shown in Table 2. Nevertheless, these rate constants are unobservable but only obtained using the transition-state theory. This is because the intramolecular hydrogen bonding (S···HO) in SC'' is weak and preferably transformed to SC'''. The reaction enthalpies for the first and second rotameric transformations are in orders: OC → OC'' < ON → ON'' < SC → SC'' < SN → SN'' and SC'' → SC''' < SN'' → SN''' < OC'' → OC''' < ON'' → ON''', respectively. And the activation energies for the first and the second rotameric transformations are in orders: SC → SC'' < ON → ON'' < OC → OC'' < SN → SN'' and SC'' → SC''' < SN'' → SN'''

$< ON'' \rightarrow ON''' < OC'' \rightarrow OC'''$, respectively. All studied compounds, the reaction enthalpies and activation energies for the first rotameric transformation are always higher than for the second rotameric transformation. The reaction enthalpies and activation energies for the first and second rotameric transformations of compounds in HPyBX series are higher than the corresponding compounds in HBX series. Rate constants at 298 K for the first and second rotameric processes are in orders: $SC \rightarrow SC'' > ON \rightarrow ON'' > OC \rightarrow OC'' > SN \rightarrow SN''$ and $SC'' \rightarrow SC''' > SN'' \rightarrow SN''' > OC'' \rightarrow OC''' > ON'' \rightarrow ON'''$, respectively. It was found that rate constants for the second rotamerization for all compounds are obviously higher than that for the first rotamerization because their activation energies are pretty low.

The activation energies for the tautomerization processes via the water-assisted intramolecular proton transfer as transition states TS_NCW_NCW', TS_OCW_OCW', TS_ONW_ONW', TS_SNW_SNW' are lower than those obtained via the direct proton-transfer as transition states TS_NC_NC', TS_OC_OC', TS_ON_ON', TS_SN_SN' by approximate 0.08, 11.68, 0.34, and 5.87 kcal/mol, respectively.

Frontier MO energies and chemical indices

Energies of the lowest unoccupied molecular orbital (E_{LUMO}) and the highest occupied molecular orbital (E_{HOMO}), frontier molecular orbital energy gap, $\Delta E_{HOMO–LUMO}$, chemical hardness, chemical potential, and Mulliken electronegativity of all isomers of HBX and HPyBX series calculated at the B3LYP/6-311++G(d,p) level are listed in Table 3. The chemical hardness, electronic chemical potential, and electronegativity are important property to study the relative stabilities of different isomers of a molecular system. Due to the Pearson's maximum hardness principle (MHP) [43] which points out that the minimum energy structure has the maximum chemical hardness, it seems that N_{syn} form of HBI and HPyBI compounds, respectively represented NC and NN are in a good agreement with this principle, whereas N_{anti} form of HBO, HBT, HPyBO, and HPyBT compounds, respectively represented by OC'', SC'', ON'', and SN'' have maximum chemical hardness values. The relative reactivities of isomeric molecules of the compounds HBI, HBO, HBT, HPyBI, HPyBO, and HPyBT are in orders: NC' > NC, OC' > OC > OC'' ≈ OC''', SC' > SC > SC''' > SC'', NN' > NN, ON' > ON''' > ON > ON'', and SN' > SN > SN''' > SN'', respectively.

Table 3 The E_{LUMO} and E_{HOMO} energies and frontier molecular orbital energy gap, $\Delta E_{HOMO-LUMO}$ of all isomers of HBX and HPyBX series computed at the B3LYP/6-311++G(d,p) level of theory

Compounds/ Isomers	E_{LUMO}[a]	E_{HOMO}[a]	$\Delta E_{HOMO-LUMO}$[a]	η[a, b]	μ[a, c]	χ[a, d]
HBI						
NC	−1.69	−6.04	4.35	2.18	−3.86	3.86
NC'	−1.82	−5.36	3.54	1.77	−3.59	3.59
TS_NC_NC'	−1.80	−5.47	3.67	1.84	−3.63	3.63
HBO						
OC	−1.91	−6.26	4.35	2.18	−4.08	4.08
OC'	−2.07	−5.61	3.54	1.77	−3.84	3.84
OC''	−1.91	−6.29	4.38	2.19	−4.10	4.10
OC'''	−1.74	−6.12	4.38	2.19	−3.93	3.93
TS_OC_OC'	−2.18	−5.82	3.65	1.82	−4.00	4.00
TS_OC_OC''	−1.39	−6.61	5.23	2.61	−4.00	4.00
TS_OC''_OC'''	−1.74	−6.37	4.63	2.31	−4.06	4.06
HBT						
SC	−2.07	−6.21	4.14	2.07	−4.14	4.14
SC'	−2.23	−5.58	3.35	1.67	−3.91	3.91
SC''	−1.91	−6.40	4.49	2.25	−4.15	4.15
SC'''	−1.80	−6.15	4.35	2.18	−3.97	3.97
TS_SC_SC'	−2.15	−5.85	3.70	1.85	−4.00	4.00
TS_SC_SC''	−1.58	−6.53	4.95	2.48	−4.06	4.06
TS_SC''_SC'''	−1.91	−6.34	4.44	2.22	−4.12	4.12
HPyBI						
NN	−1.93	−6.18	4.25	2.12	−4.06	4.06
NN'	−2.01	−5.55	3.54	1.77	−3.78	3.78
TS_NN_NN'	−1.99	−5.77	3.78	1.89	−3.88	3.88
HPyBO						
ON	−2.15	−6.45	4.30	2.15	−4.30	4.30
ON'	−2.31	−5.88	3.57	1.78	−4.10	4.10
ON''	−2.12	−6.45	4.33	2.16	−4.29	4.29
ON'''	−2.01	−6.26	4.25	2.12	−4.14	4.14
TS_ON_ON'	−2.29	−5.96	3.67	1.84	−4.12	4.12
TS_ON_ON''	−1.52	−6.91	5.39	2.69	−4.22	4.22
TS_ON''_ON'''	−1.88	−6.53	4.65	2.33	−4.20	4.20
HPyBT						
SN	−2.23	−6.40	4.16	2.08	−4.31	4.31
SN'	−2.42	−5.80	3.37	1.69	−4.11	4.11
SN''	−1.99	−6.64	4.65	2.33	−4.31	4.31
SN'''	−2.04	−6.26	4.22	2.11	−4.15	4.15
TS_SN_SN'	−2.40	−5.91	3.51	1.76	−4.15	4.15
TS_SN_SN''	−1.71	−6.83	5.12	2.56	−4.27	4.27
TS_SN''_SN'''	−2.10	−6.48	4.38	2.19	−4.29	4.29

[a] In eV

[b] Chemical hardness, $\eta = (\Delta E_{HOMO-LUMO})/2$

[c] Electronic chemical potential, $\mu = (E_{HOMO} + E_{LUMO})/2$

[d] The Mulliken electronegativity, $\chi = -(E_{HOMO} + E_{LUMO})/2$

Conclusions

The B3LYP/6-311++G(d,p) optimized structures of all isomers of HBI, HBO, HBT, HPyBI, HPyBO, and HPyBT compounds were obtained. Four isomers for each compound of HBO, HBT, HPyBO, HPyBT and three transition states of their transformations, two isomers for each compound of HBI, HPyBI and one transition state were found. The relative stabilities of isomers of the HBO, HBT, HPyBO, HPyBT, HPyBI, and HBI are in orders: $OC > OC'' > OC''' > OC'$, $SC > SC''' > SC'' > SC'$, $ON > ON'' > ON' > ON'''$, $SN > SN' > SN'' > SN'''$, $NN > NN'$, and $NC > NC'$, respectively. Energy gaps for all isomers, derived from their frontier orbital energies were obtained. Energetics, thermodynamic properties, rate constants, and equilibrium constants of all related transformations were determined at 298 K.

References

1. Lim S-J, Seo J, Park SY (2006) J Am Chem Soc 128:14542–14547. doi:10.1021/ja0637604
2. Ma DG, Liang FS, Wang LX, Lee ST, Hung LS (2002) Chem Phys Lett 358:24–28. doi:10.1016/S0009-2614(02)00546-8
3. Paterson MJ, Robb MA, Blancafort L, DeBellis AD (2005) J Phys Chem A 109:7527–7537. doi:10.1021/jp051108+
4. Klymchenko AS, Pivovarenko VG, Demchenko AP (2003) J Phys Chem A 107:4211–4216. doi:10.1021/jp027315g
5. Sarkar M, Ray JG, Sengupta PK (1996) Spectrochim Acta A Mol Biomol Spectrosc 52:275–278. doi:10.1016/0584-8539(95)01622-8
6. Klymchenko AS, Demchenko AP (2002) Langmuir 18:5637–5639. doi:10.1021/la025760x
7. Das K, Sarkar N, Majumdar D, Bhattacharyya K (1992) Chem Phys Lett 198:443–448. doi:10.1016/0009-2614(92)80025-7
8. Das K, Sarkar N, Ghosh AK, Majumdar D, Nath DN, Bhattacharyya K (1994) J Phys Chem 98:9126–9132. doi:10.1021/j100088a006
9. Mosquera M, Penedo JC, Rios Rodriguez MC, Rodriguez-Preito F (1996) J Phys Chem 100:5398–5407. doi:10.1021/jp9533638
10. Rios MA, Rios MC (1998) J Phys Chem 102:1560–1567
11. Rios MA, Rios MC (1995) J Phys Chem 99:12456–12460. doi:10.1021/j100033a014
12. Ohshima A, Momotake A, Nagahata R, Arai T (2005) J Phys Chem A 109:9731–9736. doi:10.1021/jp053702p
13. Fernandez-Ramos A, Rodriguez-Otero J, Rios MA, Soto J (1999) J Mol Struct THEOCHEM 489:255–262. doi:10.1016/S0166-1280(99)00062-7
14. Lochbrunner S, Stock K, Riedle E (2004) J Mol Struct 700:13–18. doi:10.1016/j.molstruc.2004.01.038
15. Abou-Zied OK, Jimenze R, Romesberg FE (2001) J Am Chem Soc 123:4613–4614. doi:10.1021/ja003647s
16. Dupradeau FY, Case DA, Yu C, Jimenez R, Romesberg FE (2005) J Am Chem Soc 127:15612–15617. doi:10.1021/ja054607x
17. Wang H, Zhang H, Abou-Zied OK, Yu C, Romesberg FE, Glasbeek M (2003) Chem Phys Lett 367:599–608. doi:10.1016/S0009-2614(02)01741-4
18. Chou P-T, Studer SL, Martinez ML (1991) Chem Phys Lett 178:393–398. doi:10.1016/0009-2614(91)90271-A
19. Chou P-T, Martinez ML, Studer SL (1992) Chem Phys Lett 195:586–590. doi:10.1016/0009-2614(92)85567-T
20. Lochbrunner S, Wurzer AJ, Riedle E (2003) J Phys Chem A 107:10580–10590. doi:10.1021/jp035203z
21. Vivie-Riedle R, De Waele V, Kurtz L, Riedle E (2003) J Phys Chem A 107:10591–10599. doi:10.1021/jp035204r
22. Rodriguez-Preito F, Rios Rodriguez MC, Mosquera Gonzalez M, Rios Fernandez MA (1994) J Phys Chem 98:8666–8672. doi:10.1021/j100086a014
23. Vazquez SR, Rodriguez MCR, Mosquera M, Rodriguez-Preito F (2007) J Phys Chem A 111:1814–1826. doi:10.1021/jp0653813
24. Becke AD (1993) J Chem Phys 98:5648–5652. doi:10.1063/1.464913
25. Lee C, Yang W, Parr RG (1988) Phys Rev B 37:785–789. doi:10.1103/PhysRevB.37.785
26. Frisch MJ, Trucks GW, Schlegel HB, Scuseria GE, Robb MA, Cheeseman JR, Montgomery JA Jr, Vreven T, Kudin KN, Burant JC, Millam JM, Iyengar SS, Tomasi J, Barone V, Mennucci B, Cossi M, Scalmani G, Rega N, Petersson GA, Nakatsuji H, Hada M, Ehara M, Toyota K, Fukuda R, Hasegawa J, Ishida M, Nakajima T, Honda Y, Kitao O, Nakai H, Klene M, Li X, Knox JE, Hratchian HP, Cross JB, Adamo C, Jaramillo J, Gomperts R, Stratmann RE, Yazyev O, Austin AJ, Cammi R, Pomelli C, Ochterski JW, Ayala PY, Morokuma K, Voth GA, Salvador P, Dannenberg JJ, Zakrzewski VG, Dapprich S, Daniels AD, Strain MC, Farkas O, Malick DK, Rabuck AD, Raghavachari K, Foresman JB, Ortiz JV, Cui Q, Baboul AG, Clifford S, Cioslowski J, Stefanov BB, Liu G, Liashenko A, Piskorz P, Komaromi I, Martin RL, Fox DJ, Keith T, Al-Laham MA, Peng CY, Nanayakkara A, Challacombe M, Gill PMW, Johnson B, Chen W, Wong MW, Gonzalez C, Pople JA (2006) Gaussian 03, Revision C.02. Gaussian Inc., Wallingford, CT
27. Sabin JR, Trickey SB, Apell SP, Oddershede J (2000) Int J Quantum Chem 77:358. doi:10.1002/(SICI)1097-461X(2000)77:1<358::AID-QUA35>3.0.CO;2-D
28. Koopmans T (1933) Physica 1:104–113. doi:10.1016/S0031-8914(34)90011-2
29. Wanno B, Ruangpornvisuti V (2005) Chem Phys Lett 415:176–182. doi:10.1016/j.cplett.2005.08.141
30. Wanno B, Ruangpornvisuti V (2006) J Mol Struct 787:76–89. doi:10.1016/j.molstruc.2005.11.006
31. Wanno B, Ruangpornvisuti V (2006) J Mol Struct THEOCHEM 766:159–164. doi:10.1016/j.theochem.2006.04.011
32. Wanno B, Ruangpornvisuti V (2006) J Mol Struct THEOCHEM 775:113–120. doi:10.1016/j.theochem.2006.08.017
33. Navakhun K, Ruangpornvisuti V (2006) J Mol Struct THEOCHEM 772:23–30. doi:10.1016/j.theochem.2006.06.013
34. Navakhun K, Ruangpornvisuti V (2007) J Mol Struct THEOCHEM 806:145–153. doi:10.1016/j.theochem.2006.11.016
35. Keawwangchai S, Tuntulani T, Ruangpornvisuti V (2007) J Mol Struct 832:16–25. doi:10.1016/j.molstruc.2006.07.039
36. Ruangpornvisuti V (2007) Struct Chem 18:977–984. doi:10.1007/s11224-007-9258-7
37. Thipyapong K, Ruangpornvisuti V (2008) J Mol Struct 891:1–10. doi:10.1016/j.molstruc.2008.02.004
38. Wigner EZ (1932) Phys Chem B 19:203–204
39. Hirschfelder JO, Wigner E (1939) J Chem Phys 7:616–628. doi:10.1063/1.1750500

40. Bell RP (1980) The tunnel effect in chemistry. Chapman and Hall, London
41. Leffler JE (1953) Science 117:340–341. doi:10.1126/science.117.3039.340
42. Hammond GS (1955) J Am Chem Soc 77:334–338. doi:10.1021/ja01607a027
43. Pearson RG (2001) Hard and soft acids and bases. Dowden (Hutchison & Ross), Stroudsburg, PA